Carbon Nanotube Fiber

4

CFD-enabled Optimization for Highly Efficient Purging in Glovebox used for CNT Fiber Production

Rajath Alexander*, Amit Kaushal and Kinshuk Dasgupta

Glass & Advanced Materials Division, Bhabha Atomic Research Centre (BARC), Trombay – 400085, INDIA

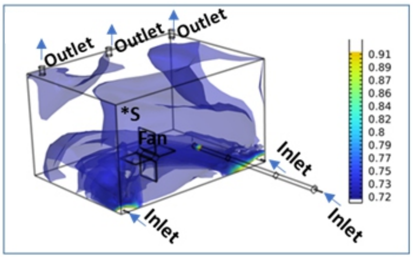

Iso-surface plot of argon concentration

ABSTRACT

Glovebox is an important and necessary instrument required for the processing and handling of dangerous and highly reactive materials. Purging of glovebox with inert gas is necessary for the safe operation, but this is a highly inefficient process owing to the channeling and dead zone formation. In this work we have carried out computational fluid dynamics (CFD) simulation of a glove box used for carbon nanotube fiber (CNT fiber) production to understand the flow profile. The flow profile was used to optimize the inlet and the outlet locations in the glovebox. The CFD-enabled strategic placement of inlet and outlet in the glove box helps in lowering the gas requirement by 40%. The effect of rotating fan in the glove box was also investigated. The rotating fan helped in mixing the inert gas with existing air in the glovebox and eliminated the dead zone formation thereby enhancing the purging efficiency. The parameters from the CFD simulation were also successfully validated using experiments in actual glove box.

KEYWORDS: *Computational Fluid Dynamics (CFD), Carbon nanotube fiber, Glovebox*

Introduction

Glovebox is an ineluctable instrument in recent times in the field of engineering for the fabrication of advanced materials, which requires stringent environmental control for processing. Glovebox makes handling and processing of dangerous and reactive material possible. Radioactive material like plutonium is exclusively processed in the glovebox for fuel fabrication and processes involved in reprocessing of fuel [1]. One of the major commercial applications of the glovebox is its use in the fabrication of Li-ion batteries. Glovebox for making the battery is operated at a highly stringent condition where oxygen and moisture is maintained at less than 1 ppm [2]. Gloveboxes are maintained in an inert atmosphere by purging inert gas like argon and nitrogen when handling reactive material [2]. Glovebox is also maintained at a slight positive pressure to prevent the ingress of atmospheric gas. The positive pressure is necessary as rubber gloves tend to permeate gases [3]. The glovebox achieves a high level of purity by recirculating the inert gas through a regenerative system [4]. In the regenerative system, inert gas is passed through heated getter material like copper.

The glovebox used for the synthesis of CNT fiber is maintained at atmospheric pressure in comparison to other gloveboxes which are maintained generally at positive pressure. Some glovebox are also maintained in negative pressure when handling toxic and radioactive material as it prevents the leakage in the environment [5]. The glovebox that operating at positive pressure requires continuous purging of inert gas to maintain safe working conditions. The glovebox used for the synthesis of CNT fiber requires to be evacuated after every production run for the collection of CNT fiber and for servicing the system. This working procedure makes the consumption of argon gas extremely high compared to conventional gloveboxes where the processed material can be recovered without evacuating the entire glovebox through an anti-chamber. This makes argon gas the most expensive consumable in the synthesis of CNT fiber.

In this work, we have utilized computational fluid dynamics (CFD) to lower argon consumption by improving purging efficiency by optimizing inlet and outlet locations. The feasibility of using a fan for enhancing purging efficiency was also assessed.

Experimental Section

The CFD analysis was carried out on a glove with dimensions of 1200 mm length, 900 mm width, and 700 mm height with an attached horizontal tube furnace. The tube size in the furnace is 1000 mm in length and 45 mm in diameter. The flow in the system was modeled using k-ε turbulence model along with Reynolds Average Navier Stokes equations. The governing equations of the model are given below in Eqs (1-7):

$$\rho(\boldsymbol{u}.\nabla)\boldsymbol{u} = \nabla.[-p\boldsymbol{I} + \boldsymbol{K}] + \boldsymbol{F} \quad (1)$$

$$\nabla.(\rho\boldsymbol{u}) = 0 \quad (2)$$

$$\boldsymbol{K} = (\mu + \mu_T)(\nabla\boldsymbol{u} + (\nabla\boldsymbol{u})^T) - \frac{2}{3}(\mu + \mu_T)(\nabla.\boldsymbol{u})\boldsymbol{I} - \frac{2}{3}\rho k\boldsymbol{I} \quad (3)$$

$$\rho(\boldsymbol{u}.\nabla)k = \nabla.\left[\left(\mu + \frac{\mu_T}{\sigma_k}\right)\nabla k\right] + P_k - \rho\epsilon \quad (4)$$

$$\rho(\boldsymbol{u}.\nabla)k = \nabla.\left[\left(\mu + \frac{\mu_T}{\sigma_\varepsilon}\right)\nabla\epsilon\right] + C_{\epsilon 1}\frac{\epsilon}{k}P_k - C_{\epsilon 2}\rho\frac{\epsilon^2}{k} \quad (5)$$

$$\mu_T = \rho C_\mu \frac{k^2}{\epsilon} \quad (6)$$

$$P_k = \mu_T\left[\nabla\boldsymbol{u}:(\nabla\boldsymbol{u} + (\nabla\boldsymbol{u})^T) - \frac{2}{3}(\nabla.\mu)^2\right] - \frac{2}{3}\rho k\nabla.\boldsymbol{u} \quad (7)$$

*Author for Correspondence: Rajath Alexander
E-mail: alexander@barc.gov.on

The change in the composition of gases in the glovebox was modeled using species transport equation. The governing equation is given below in Eq (8).

$$\rho\frac{\partial}{\partial x}(\omega_i) + \rho(\mathbf{u}.\nabla)\omega_i = \nabla.\left(\rho D_{T,i}\nabla\omega_i + \rho\omega_i D_{T,i}\frac{\nabla M}{M}\right) \quad (8)$$

$$Sc_T = \left(0.58852 + 0.228\left(\frac{v_T}{v}\right) - 0.0441\left(\frac{v_T}{v}\right)\left[1 - e^{-\frac{5.165}{(v_T/v)}}\right]\right)^{-1} \quad (9)$$

$$D_{T,i} = \frac{v_T}{Sc_c}e^{(-\Gamma)} + D_{T,w}e^{(-1/\Gamma)} \quad (10)$$

$$\Gamma = \frac{0.01(l^*)^4}{(1+5l^*)} \quad (11)$$

The glovebox was purged with 80 LPM of argon and the reactor tube was purged with 4 LPM of argon. The gas was sent using a mass flow controller. The oxygen level in the system was validated using a zirconium dioxide oxygen sensor.

Result and Discussion

Single inlet outlet design

The CFD simulation result of the glove box with one inlet and one outlet is shown in Fig.1(a). It can be seen that the velocity is higher near the inlet and reduces drastically in other regions, especially in the corners away from the inlet and outlet. This can cause variations of oxygen purge time at various locations in the glove box. The streamline showing the path of the gas flow with the highest mass flow rate is given in Fig.1(b). It can be seen that the majority of gas form a single vortex without sweeping most of the volume before exiting through the outlet. This will cause the purging gas to not evacuate the gas in the majority of the region in the glove box effectively. The argon distribution in the glovebox after 20 mins of purging is given in Fig.1(c). It can be seen that the argon mole fraction in the glove box is highly non-uniform. The iso-surface plot (Fig.1(d)) shows the region with the highest purging gas content (argon mole fraction) in the initial stage of purging (20 min). It can be seen that a channel between the inlet and the outlet with argon content is present indicating high channeling. The reduction of oxygen content in the location of the oxygen sensor is given in Fig.1(e). The oxygen content from CFD and sensor reading are close to each other reaffirming the accuracy of the CFD model. It can be seen that it takes around 2 h to reach 2 vol% which is the safe working level of the glove box. The high channeling in the glovebox has been seen from the CFD simulation causing the volume of the purging gas utilized to be 35 times the volume of the glove box. This indicates the high inefficiency of the process.

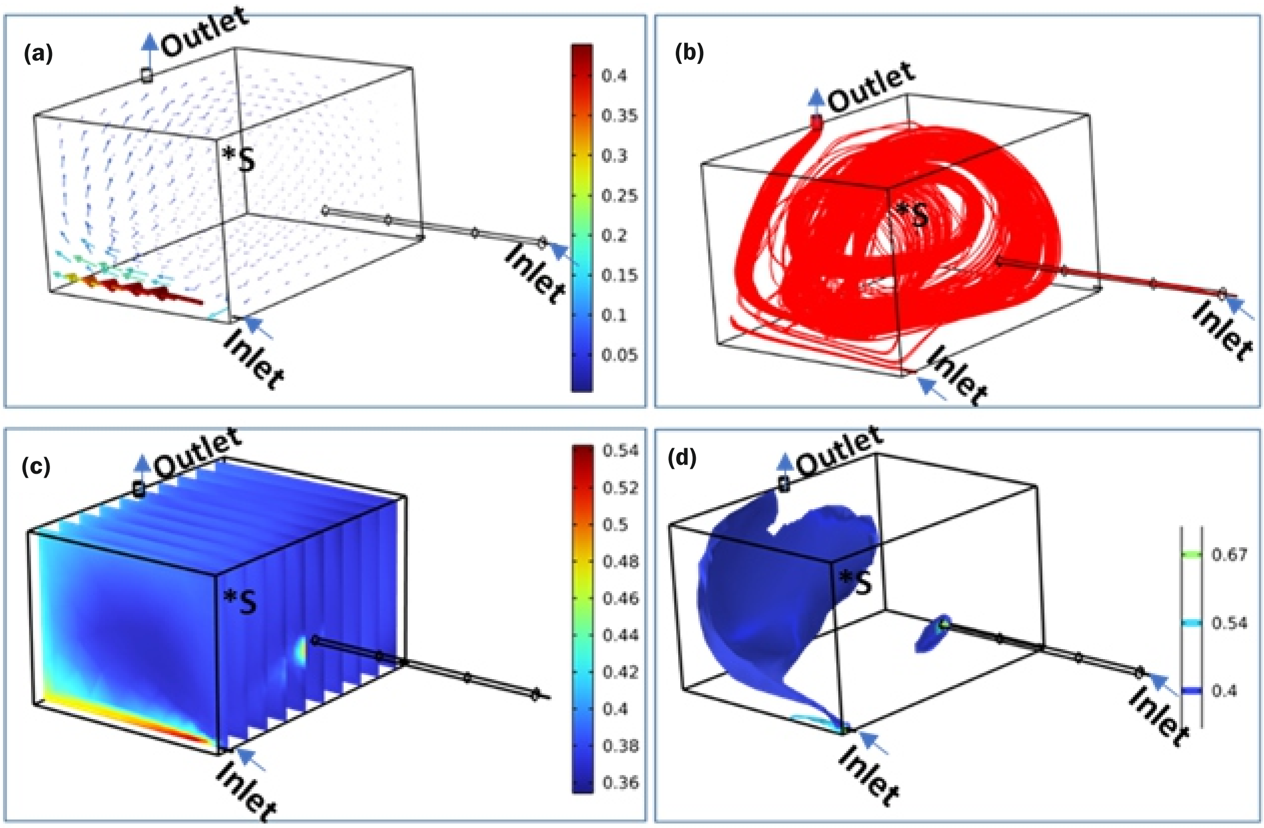

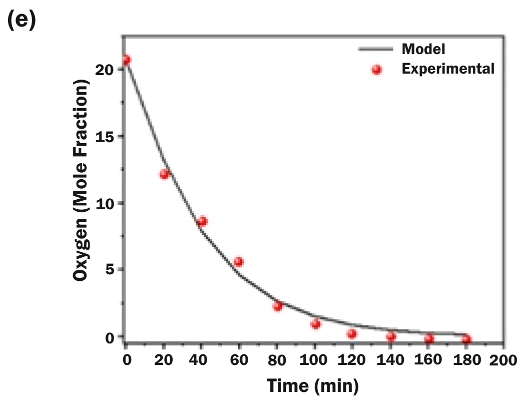

Fig.1: (a) Velocity profile in the system (S = Sensor Location).
(b) Streamline of flux of argon in the system.
(c) Argon concentration (mole fraction) in the glove.
(d) Iso-surface plot of argon concentration.
(e) Change in oxygen vol % with time.

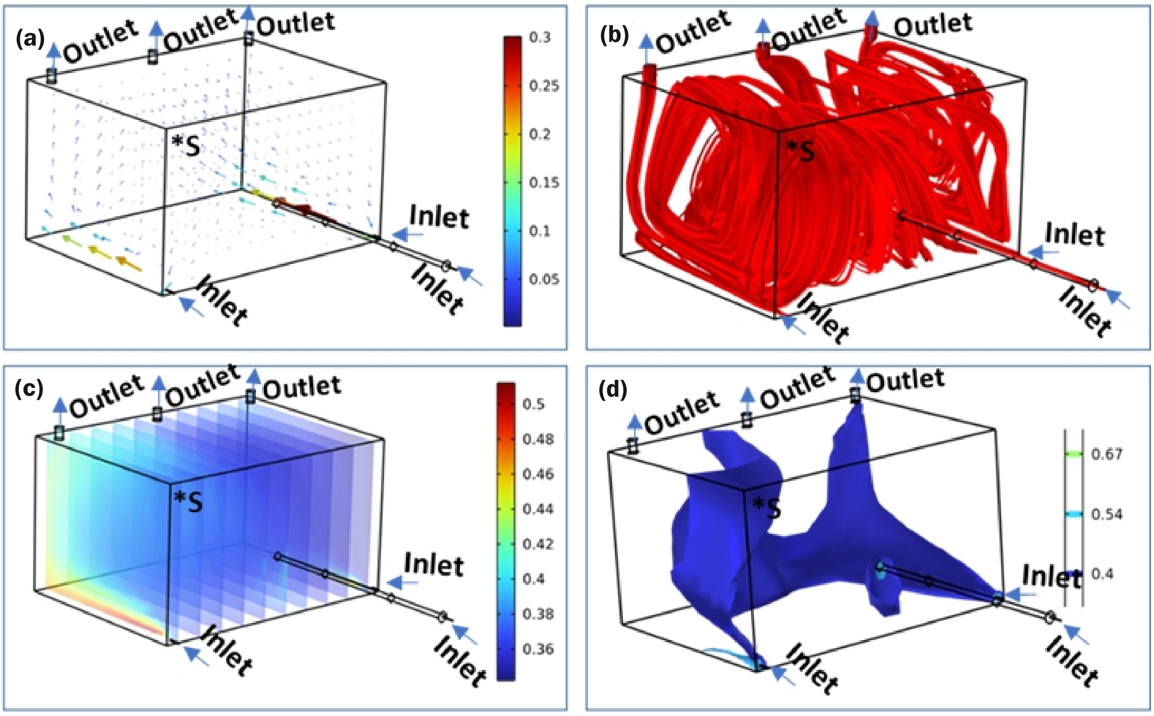

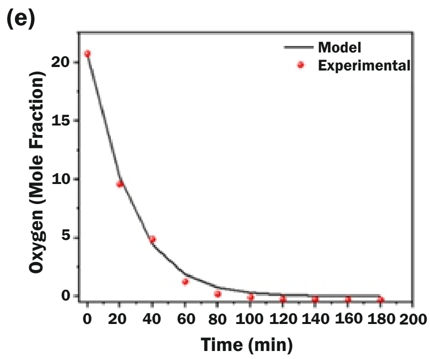

Fig.2: (a) Velocity profile in the system (S = Sensor Location).
(b) Streamline of the flux of argon in the system,
(c) Argon concentration (mole fraction) in the glove box.
(d) Iso-surface plot of argon concentration.
(e) Change in oxygen vol % with time.

Two inlet and three outlet design

To reduce channeling and dead zone as seen in the glovebox with one inlet and outlet, the glovebox box with two inlets and three outlets was utilized. The results of CFD simulation of the glovebox with two inlets and three outlets are shown in Fig.2(a). It can be seen from the velocity profile that even though maximum velocity is lower due to splitting the velocity from one inlet to two, the region which had negligible velocity in a single inlet case now has significantly higher velocity indicating better-distributed flow. The streamlines of purging gas are given in Fig.2(b). It can be seen that multiple vortexes are formed when multiple inlets and outlets are utilized. The presence of more vortex will ensure superior mixing of purging gas with initially present air in the glovebox. The argon content in the glove box in the initial stage of purging (20 min) is shown in Fig.2(c). It can be seen that argon gas distribution is not homogenous. The iso-surface (Fig.2(d)) showing the highest argon content region indicates channeling between the inlets and the outlets. In multiple inlet outlet designs, despite channeling there exist multiple paths for the gas to exit which can cause enhanced purging. The oxygen percentage at the sensor location shown in Fig.2(e) indicates that required oxygen level of 2 vol% is attained in 120 min which requires 22 times volume of gas than volume of glovebox.

Rotating fan design

As seen from the results for multi-inlet outlet design, there is a significant improvement in purging efficiency. This efficiency might further increase with an increase in the number of inlets and outlets. To achieve superior purging we have utilized a rotating fan inside the glovebox. The rotating fan was aimed to reduce the channeling and dead zone in the glovebox by enhancing the mixing in the glovebox. A four-blade impeller rotating at an rpm of 10 rpm was kept inside the glove box and experimental was performed. In CFD the rotating impeller was incorporated into the model using a moving mesh. The velocity profile (Fig.3(a)) indicates a substantial increase in velocity in the region other than the inlets. The streamlines (Fig.3(b)) of gas in the glovebox show the elimination of channeling and dead zone in the glovebox. The argon content in the glove box in the initial stage of purging is shown in Fig.3(c). It can be seen that argon gas is well distributed in the glovebox. The iso-surface of argon in the glovebox is also shown in Fig.3(d) also indicates homogenous argon concentration in the glovebox. The oxygen percentage at the sensor location shown in Fig.3(e) indicates that required oxygen level of 2 vol% is attained in 1 h which requires 17.5 times volume of gas than volume of glovebox.

Conclusions

Computation fluid dynamics was used for determining the flow profile and oxygen, argon distribution inside a glovebox with the objective of reducing the consumption of argon used as the purging gas. Channeling and large dead zone created high inefficiency in purging when only one inlet and outlet were used. The channeling and dead zone in the glove box were reduced by introducing the purging gas through two inlets and

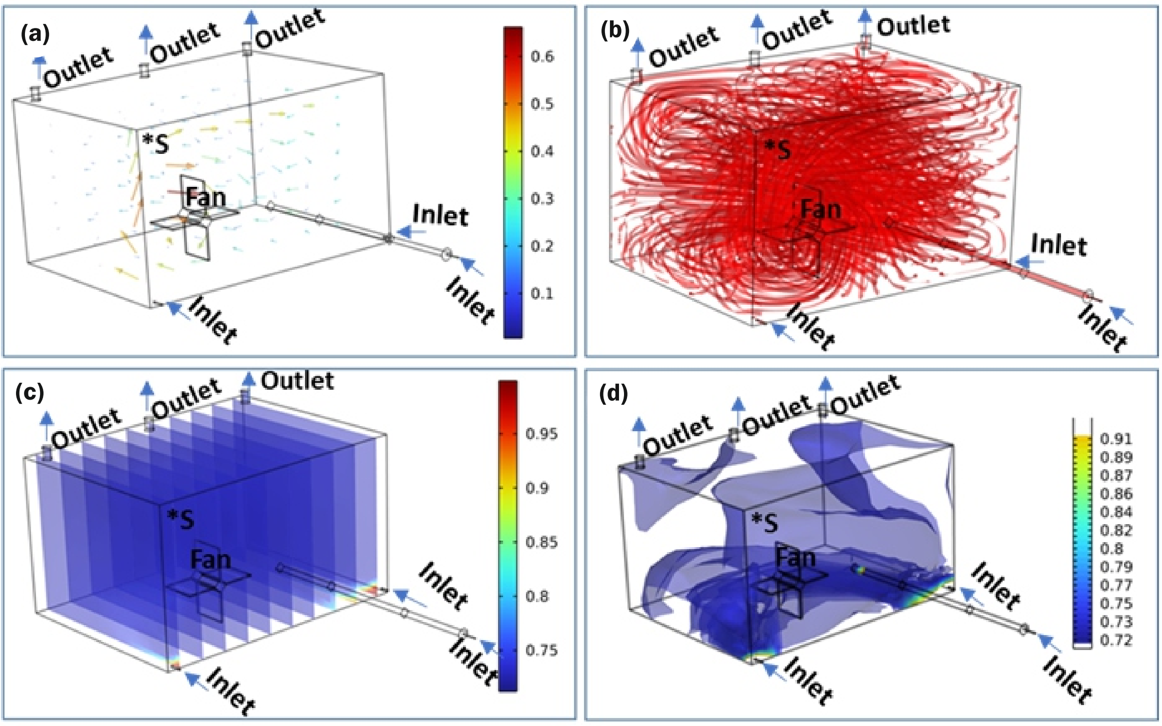

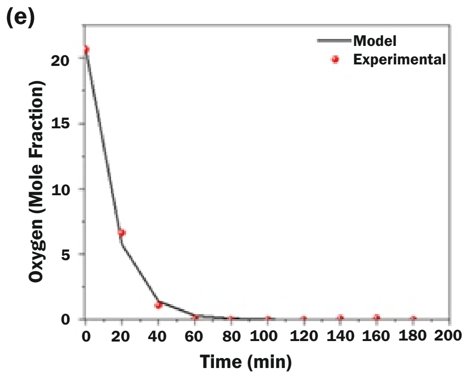

Fig.3: (a) Velocity profile in the system (S = Sensor Location).
(b) Streamline of the flux of argon in the system.
(c) Argon concentration (mole fraction) in the glovebox.
(d) Iso-surface plot of argon concentration.
(e) Change in oxygen vol % with time.

taking it out through 3 outlets outlets. Multiple inlets and outlets also increased the number of vortexes in the glovebox which enhanced the mixing and improved the purging efficiency. The introduction of a rotating fan in the glovebox further enhanced the efficiency of the purging by improving the mixing, it reduced the purging requirement by ~50 % from the initial configuration having one inlet and outlet.

References

[1] M. Rentetzi, "Determining Nuclear Fingerprints: Glove Boxes, Radiation Protection, and the International Atomic Energy Agency", Endeavour, 41 (2017) 39-50.

[2] K. Tokumitsu, H. Fujimoto, A. Mabuchi, T. Kasuh, "High capacity carbon anode for Li-ion battery: A theoretical explanation", Carbon, 37 (1999) 1599-1605.

[3] N. Vahdat, J.S. Johnson, A. Neidhardt, J. Cheng, D. Weitzman, "Permeation of Chemicals Through Glove Box Glove Materials", Applied Occupational and Environmental Hygiene, 10 (1995) 943-950.

[4] M.S. Hu, The Design and Development of Control System for High Vacuum Deoxygenated and Water-Removal Glove Box with Cycling Cleaning and Regeneration, Applied Modern Control, Intech Open, 2018.

[5] T. Fujita, K. Ohtani, M. Hayashi, M. Kozeki, T. Ide, K. Sakuno, "Earthquake resistance test of full-scale glove box", Trans. 10th SMiRT, k2 (1989) 877-882.

Notations	
ρ	Density (kg/m^3)
μ	Dynamic viscosity (kg/m.s)
$\boldsymbol{u}$	Velocity vector (m/s)
p	Pressure (Pa)
$\boldsymbol{F}$	Body force (N.m^{-3})
μ_T	Turbulent dynamic viscosity (kg/m.s)
υ	Kinematic viscosity (m^2/s)
υ_T	Turbulent kinematic viscosity (m^2/s)
k	Turbulent kinetic energy (m^2·s^{-2})
$C_\mu, C_{\epsilon 1}, C_{\epsilon 2}, \sigma_k, \sigma_\epsilon$	Model constant (0.09, 1.44, 1.92, 1.0, 1.3)
ϵ	Turbulent dissipation rate (m/s^3)
$D_{T,i}$	Turbulent diffusion coefficient (m^2/s) of ith species (i;1=Nitrogen, 2= Oxygen, and 3= Argon)
Sc_T	Turbulent Schmidt number
l^*	Characteristic length (m)
ω_i	Mass fraction of ith species (i;1=Nitrogen, 2= Oxygen, and 3= Argon)
M	Molar mass (kg)